JOURNAL OF SOLID STATE CHEMISTRY 16, 317–323 (1976)

Electrical Conduction in the Sintered Oxides of the System Bi_2O_3–BaO

TAKEHIKO TAKAHASHI, TAKAO ESAKA, AND HIROYASU IWAHARA

Department of Applied Chemistry, Faculty of Engineering, Nagoya University, Nagoya, Japan

Received April 8, 1975; in revised form July 15, 1975

The electrical conduction in various phases of the system Bi_2O_3–BaO was investigated by measurement of a–c conductivity and the EMF of oxygen gas concentration cell and observation of X-ray diffraction patterns. High oxide-ion conduction was observed in the rhombohedral phase present in 20–25-mol% BaO and hole conduction was observed in the perovskite-type phase based on $2BaO \cdot Bi_2O_3$. The oxide-ion conductivity of the 20-mol% BaO specimen was 1.1×10^{-2} mho/cm at 500°C and the contribution of electronic conductivity to total conductivity was negligibly small in air. In the remaining range of composition, where the monoclinic and rhombohedral mixed phase was found for less than 20-mol% BaO and the rhombohedral and perovskite-type structure mixed phase was observed for more than 28-mol% BaO, the conduction was attributed to oxide ion and electron hole. High oxide-ion conduction in the rhombohedral phase was considered to be due to an appreciable amount of oxide-ion vacancies in this phase.

1. Introduction

Some solid solutions having oxide ion vacancies are known as oxide-ion conductors (1–4). In these materials, the sintered oxides based on tetravalent and trivalent metallic oxides are included. In the former, calcia- or yttria-stabilized zirconia, yttria-doped thoria, and the like have been well investigated, because they have some thermodynamic and electrochemical properties suitable for high-temperature applications. The sintered oxides based on Y_2O_3 or Sm_2O_3 belong to the latter. In order to obtain these sintered oxides in a dense sintered state, they must be fired at high temperature and their oxide-ion conductivity is not always high enough for lower temperature applications. From the standpoint mentioned above, it is desirable to find materials having high oxide-ion conductivity at lower temperatures, if possible.

As previously reported by the present authors, some solid solutions based on trivalent metallic oxide, that is, Bi_2O_3 were found to be high oxide ion conductors (*5–8*). Though pure Bi_2O_3 shows high oxide-ion conductivity in the temperature range 730–825°C (mp), the charge carriers change from oxide ions to electron holes at 730°C by the phase transformation from face-centered cubic δ-Bi_2O_3 (high-temperature form) to monoclinic α-Bi_2O_3 (low-temperature form) (*9–12*). The high oxide-ion conductivity of Bi_2O_3 observed above 730°C could not be retained at lower temperature by quenching of the sample. Moreover, the δ-α phase transformation is accompanied by a large volume change, which makes the specimen collapse. Therefore, Bi_2O_3 is unable to be used practically as an oxide-ion conductor. The present authors found that the high oxide-ion conductivity was retained over a wide range of temperature, when the fcc phase corresponding to the high-temperature form of Bi_2O_3 was stabilized by adding Y_2O_3, Gd_2O_3, and WO_3 to Bi_2O_3. For example, the sample containing 25-mol% Y_2O_3 exhibits the fcc form, which shows 8.3×10^{-2} mho/cm at

600°C (*5*). This conductivity is about one order of magnitude higher than that of well-known stabilized zirconias at the corresponding temperature. Similar results were obtained in the system Bi_2O_3–WO_3 (*6*). In the system Bi_2O_3–Gd_2O_3, high oxide-ion conduction was found not only in the fcc phase but also in the rhombohedral phase (*7*).

As to oxide-ion conduction in the rhombohedral phase, the authors also found that the rhombohedral phase in the system Bi_2O_3–CaO and Bi_2O_3–SrO showed high oxide-ion conduction (*8*). Levin and Roth reported the presence of the rhombohedral phase in the systems Bi_2O_3–CaO, Bi_2O_3–SrO, and Bi_2O_3–BaO (*13*). The present authors observed that the rhombohedral phase containing SrO, the cationic radius of which is larger than that of CaO, showed somewhat higher oxide-ion conductivity than that containing CaO (*8*). As Ba^{2+} has a larger cationic radius than Sr^{2+}, the rhombohedral phase in the system Bi_2O_3–BaO was expected to have higher oxide-ion conductivity than that in the system Bi_2O_3–SrO. From this point of view, the oxide-ion conduction in this material was investigated. Furthermore, as the phase diagram by Levin et al. is limited in a narrow range of composition (~ 22-mol% BaO), the authors also investigated the relationship between the electrical conduction and the phase in the system Bi_2O_3–BaO over a wide range of composition.

2. Experimental

2.1. Preparation of Samples

The starting materials used were bismuth sesquioxide and barium nitrate. Bismuth sesquioxide was obtained by thermal decomposition of $Bi(NO_3)_3 \cdot 5H_2O$ (JIS special grade) at 700°C and barium nitrate was refined twice by recrystallization.

A mixture of finely ground starting materials was calcined in air at about 600°C for a few hours, in order to decompose $Ba(NO_3)_2$ into BaO, and kept at 700–740°C for 10 hr. The pre-fired specimens were powdered and molded under a pressure of 3 ton/cm^2 into the shape of cylinder (4–6 mmϕ × 8–12 mm) or disk (12 mmϕ × 2–3 mm). The molded samples were sintered again in air at 700–740°C for 10 hr. To obtain dense samples, the sintering temperature was raised as the content of BaO increased.

Samples thus prepared were well sintered and the porosity, calculated from the ratio of the density of the sintered sample to that of the powdered one, was less than 7%, which was corrected for in the various electrical measurements. The color of specimens was yellowish for 10–30 mol% BaO, changed to brown with increasing BaO content, and became black for more than 50-mol% BaO specimens.

The crystal structure of specimens was identified by X-ray diffraction patterns using CuKα radiation with a nickel filter. The lattice parameters were calculated from the diffraction angles of each peak obtained by slow scanning speed (1°/4 min^{-1}) using $Pb(NO_3)_2$ as internal standard. The densities of several samples were measured at 25°C by the standard pycnometric method using *n*-butanol.

2.2. Measurement of Ionic Conduction

The ionic conduction in the specimens was examined by measuring the electrical conductivity and the EMF of the oxygen gas concentration cells using the specimen disks as electrolytes.

Electrical conductivity was measured in the temperature range 300–700°C under various partial pressures of oxygen using a two-probe a-c method. The frequency used was 10 kHz. Cylindrical specimens were silvered on their faces and held between two alumina sample holders which were placed in an electric furnace. The temperature was controlled with an accuracy of $\pm\frac{1}{2}$°C during the experiments. Contact resistance and surface conduction of the samples could be neglected in these conductivity measurements, because cylindrical samples of different sizes gave equal specific conductivities within experimental errors.

To determine the ionic transference number, the EMF of the following oxygen concentration cell was measured,

$$O_2(P_{O_2}, a), Ag|\text{specimen disk}|Ag, O_2(P_{O_2}, c) \quad (1)$$

where $P_{O_2}, a = 0.21$ atm and $P_{O_2}, c = 1.00$ atm. The design of the cell, as well as the general procedure and the theory for EMF measurement, has been described in detail elsewhere (*14*).

3. Results and Discussion

3.1. X-Ray Diffraction

Figure 1 shows the X-ray diffraction patterns of specimens that were cooled slowly from firing temperature. The specimens containing less than 20-mol% BaO indicated the mixed patterns of monoclinic and rhombohedral phase, and the single rhombohedral phase was observed for 20–25-mol% BaO. A new phase appeared in addition to the rhombohedral phase for more than 28-mol% BaO. This phase was based on the compound $2BaO \cdot Bi_2O_3$, which crystallized in the perovskite crystal structure.

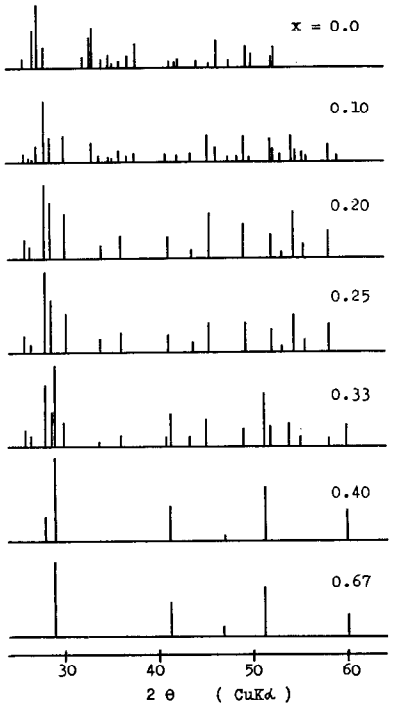

FIG. 1. X-ray diffraction patterns of $(Bi_2O_3)_{1-x}(BaO)_x$.

3.2. Ionic Conductivity

The variation of conductivity with temperature measured in air for polycrystalline specimens having BaO concentration between 10 and 67-mol% is represented in Fig. 2. The temperature dependence of the conductivity of pure Bi_2O_3 is shown in the same figure by the dashed line, which shows an abrupt conductivity change at 730°C, indicating that Bi_2O_3 is transformed from monoclinic into fcc at the corresponding temperature.

The specimens containing BaO showed conductivity behavior somewhat similar to that of pure Bi_2O_3. However, the degree of jump in the conductivity was small compared with pure Bi_2O_3 and the jumping temperature was about 150°C lower than that of pure Bi_2O_3. As described in the next section, these conductivity jumps were considered to be due to the transition into the high-temperature phase. The 33-mol% BaO specimen showed little break in conductivity, which might be caused by partial freezing of the high-temperature phase. Therefore, the conductivity of this sample at lower temperatures (dotted line) may represent the value

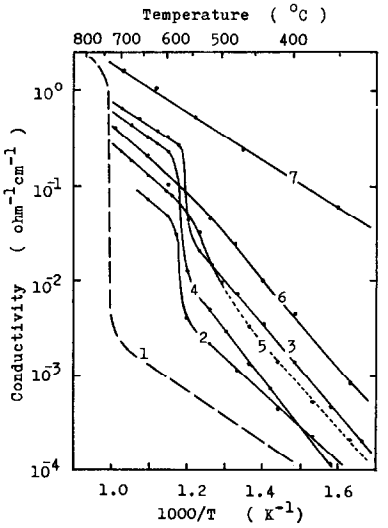

FIG. 2. Conductivity versus reciprocal of absolute temperature curves for $(Bi_2O_3)_{1-x}(BaO)_x$in air. 1, $x = 0.0$; 2, $x = 0.10$; 3, $x = 0.20$; 4, $x = 0.25$; 5, $x = 0.33$; 6, $x = 0.50$; 7, $x = 0.67$.

in the metastable state and will decrease considerably after infinite time. Arrhenius plots of 50- and 67-mol% BaO specimens showed alomst linear variation over the wide range of temperature measured. The activation energy for conduction in the rhombohedral single phase was 0.92 eV below 580°C and 0.48 eV above 580°C, and that in the perovskite single phase was 0.50 eV over the whole range of temperature measured.

The charge carriers in these conductors were investigated by measuring the EMF of the oxygen gas concentration cell using the specimen disks as the electrolytes. Figure 3 represents the ratio of measured EMF to the theoretical one. Anode gas was air (1 atm) and cathode gas was pure oxygen (1 atm). The values of E/E_0 for the rhombohedral single phase (20–25 mol% BaO) are above 0.95 for the whole range of temperature examined, indicating that ionic conduction is predominant, while E/E_0 is near zero for pure Bi_2O_3 (<730°C) and 67-mol% BaO specimen, indicating that the α-phase and perovskite-type compound are electronic-predominant conductors. As shown for 15-, 33-, and 40-mol% BaO in the same figure, E/E_0 for the mixed phase is smaller than unity because of the co-presence of ionic and electronic conduction. However, E/E_0 is near unity above 600°C in the rhombohedral-rich phase, for example, 15- and 33-mol% BaO, indicating that the high conductivity phase above 580°C is predominantly an ionic conductor.

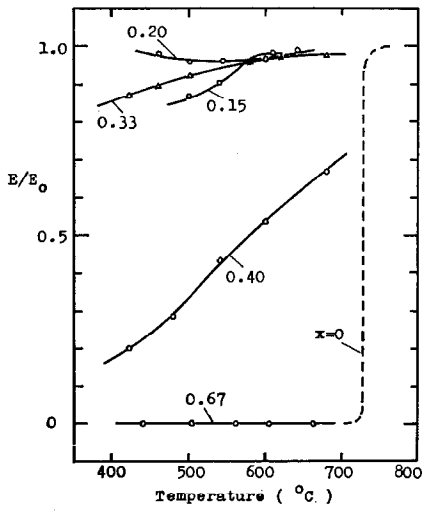

FIG. 3. Ratio of the measured EMF (E) to the theoretical value (E_0) of the following cell: O_2 (0.21 atm), $Ag|(Bi_2O_3)_{1-x}(BaO)_x|Ag, O_2$ (1.0 atm).

Steady current could be drawn from these oxygen concentration cells. The d-c conductivity calculated from the i–V relation of the cell was almost comparable to the value measured by a-c bridge. This result denotes that both electrodes act as oxygen-gas electrode reversibly and that the conductive species of the specimens are oxide ions. Therefore, the 20- and 25-mol% BaO specimens in Fig. 2 represent oxide-ion conductivity.

In the composition ranges indicating $E/E_0 < 0.9$ in Fig. 3, a correct ionic transference number cannot always be determined from E/E_0, since the electronic conduction sometimes causes electrode polarization. Therefore, E/E_0 in these cases was compared with the value obtained by the following method (*15*).

When a gas concentration cell shows a lower EMF than the theoretical value (E_0), E_0 is applied to the cell from an outer source in charging polarity. In this condition, no ionic current passes through the specimen and the observed current (i_e) is ascribed to electron. It is obvious, then, that the polarization effect of the oxygen electrode reaction need not be considered. The electronic conductivity (σ_e) in this case can be given as

$$\sigma_e = i_e/E_0. \tag{2}$$

The transference number of ions (t_i) is defined as

$$t_i = 1 - (\sigma_e/\sigma), \tag{3}$$

where σ is the total conductivity of specimen disk. Using Eq. (2), Eq. (3) can be rewritten as

$$t_i = 1 - (i_e/\sigma E_0). \tag{4}$$

As σ can be measured by an a-c bridge with sufficiently high frequency, one can obtain the t_i from i_e. For example, $t_i = 0.72$ was calculated for the 40-mol% BaO sample at 680°C, which was somewhat larger than the value obtained directly from EMF measurement

($E/E_0 = 0.67$). For the specimen which shows higher E/E_0 value than 0.9, the value of t_i thus calculated coincided with E/E_0 within experimental errors. These results indicated that the electrode reaction of oxygen gas proceeded reversibly.

Figure 4 shows the conductivity of the specimens measured in various oxygen atmospheres of air–argon mixture. When the concentration of movable ions is sufficiently high, ionic conductivity is independent of oxygen partial pressure, whereas the conductivity of electron holes or excess electrons shows the pressure dependence. This is generally expressed as

$$\sigma = \sigma_{ion} + A \cdot P_{O_2}^{1/m} + B \cdot P_{O_2}^{-1/n}, \qquad (5)$$

where A and B are constants and m and n are positive integers (*16*). The conductivity of the 25-mol% BaO sample does not show the pressure dependence above and below the temperature at which the conductivity changes abruptly. This means that the ionic conduction is predominant in the rhombohedral phase. The 10- and 40-mol% BaO samples show the contribution of hole conduction at 500°C, while the 10-mol% BaO sample exhibits the predominant ionic conduction at 600°C. These results correspond to the relation obtained from E/E_0.

The relation between the electrical conduction and the composition can be summarized as follows: (1) The specimens having BaO content less than 20 mol% show the monoclinic and rhombohedral mixed phase. Charge carriers are electron holes in the monoclinic phase, and oxide ions in the rhombohedral phase. The conductivity increases with increasing BaO contents. (2) The specimens having 20–25 mol% BaO form the rhombohedral solid solution, in which oxide-ion conduction predominates. The oxide-ion conductivity of the 20-mol% BaO sample at 500°C is 1.1×10^{-2} mho/cm, which is about one order of magnitude higher than that of stabilized zirconias. In the rhombohedral single phase, the oxide-ion conductivity decreases with increasing content of BaO, that is, the lower the content of added oxide, the higher the oxide-ion conductivity. This is the same tendency that was observed in the other solid solution based on Bi_2O_3 (*5–7*). (3) The specimens having more than 28-mol% BaO show the rhombohedral and perovskite-type structure mixed phase. Electrical conduction is ascribed to the oxide ions in the rhombohedral phase and the electron holes in the perovskite-type phase. The hole conductivity of the perovskite-type compound $2BaO \cdot Bi_2O_3$ is noticeably higher than the ionic conductivity of the rhombohedral phase.

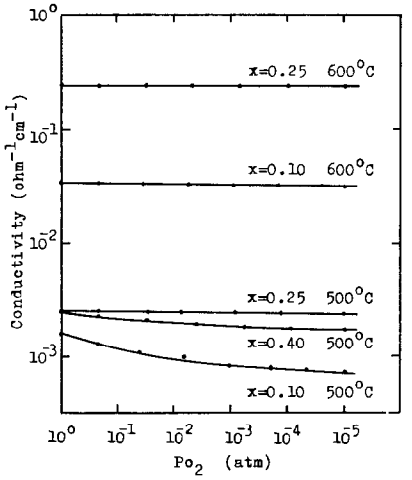

FIG. 4. Conductivity versus oxygen partial pressure relation of $(Bi_2O_3)_{1-x}(BaO)_x$.

3.3. Abrupt Change of Conductivity

Some specimens showed an abrupt change of conductivity at about 580°C (Fig. 2). Though this change was found to correspond to an endothermic change by DTA, an obvious difference in the high-temperature X-ray diffraction patterns was not observed over a measuring temperature range up to 700°C. If a liquid phase intervenes in a solid phase, a similar result may be obtained. However, the finely powdered specimen showed neither sintering nor crystal growing even after firing at 650°C, which suggests no partial melting. Careful investigation of X-ray patterns of annealed and quenched samples showed that (222), (333), (444), and (555) peaks of annealed rhombohedral phase grew strong. Accordingly, it is rational to consider that the abrupt change of conductivity in Fig. 1 is ascribed to some configurational change of atoms in the rhombohedral phase.

3.4. *Oxygen-Deficient Lattice in the Rhombohedral Phase*

In general, oxide-ion conduction is considered to be caused by the migration of oxygen ions via oxygen vacancies present in the crystal (*17*). As an appreciable amount of oxide-ion vacancies was expected to be present in the high conductive phase of the system Bi_2O_3–BaO, the oxygen-deficient lattice in the rhombohedral phase of 20–25 mol% BaO was investigated.

The lattice parameters (Table I) obtained from X-ray diffraction were used for calculation of the theoretical densities. The valencies of cations (Bi^{3+} and Ba^{2+}) were considered not to change during the formation of the rhombohedral phase, because no change in mass was observed by thermogravimetry. Using the same procedure as that reported on the system Bi_2O_3–SrO by Sillén and Aurivillius (*18*), the authors calculated X-ray densities, in which a defect structure having oxygen vacant sites was assumed. The X-ray densities were 8.50 ± 0.05 g/cm^3 for the 10-mol% BaO sample and 8.39 ± 0.05 g/cm^3 for the 25-mol% BaO sample, in agreement with the pycnometric densities 8.37 ± 0.10 and 8.25 ± 0.10 g/cm^3, respectively, within experimental errors. As a result, the rhombohedral phase was taken to have an appreciable amount of oxygen vacancies, and consequently the high oxide-ion conduction in this phase was attributed to the migration of oxygen vacancies as observed in other oxide-ion conductors.

3.5. *Formation of Perovskite-Type Cubic Structure*

The specimen $2BaO \cdot Bi_2O_3$ showed an X-ray diffraction pattern corresponding to the perovskite structure, which is generally represented as ABO_3 where A is a divalent or trivalent metal and B is a tetravalent or trivalent metal. If Bi is trivalent and Ba is divalent, the unit cell of the above perovskite-type compound should be $BaBiO_{2.5}\square_{0.5}$. Although these oxygen vacant sites were reported to be filled by oxygen on firing in oxygen atmosphere (*19*, *20*), the sample sintered in air or in lower oxygen pressure was considered to have some parts of oxygen vacant sites. And the crystal structure was considered to change from triclinic perovskite $BaBiO_3$ to cubic perovskite $BaBiO_{3-\alpha}$. The relation between defect structure and oxide-ion conduction is not under investigation.

TABLE I

UNIT CELL PARAMETERS OF THE RHOMBOHEDRAL PHASE IN THE SYSTEM Bi_2O_3–BaO

BaO (mol%)	a (Å)	$\cos\alpha$	V (Å^3)
20	9.774 ± 0.005	0.9165 ± 0.0005	131.2 ± 0.9
25	9.779 ± 0.004	0.9165 ± 0.0007	131.5 ± 0.9

4. Conclusion

In the system Bi_2O_3–BaO, there exist rhombohedral solid solution for 20–25-mol% BaO and perovskite-type compound $BaBiO_{3-\alpha}$. The rhombohedral single phase is a high oxide-ion conductor under ordinary oxygen pressure. Especially the specimen containing 20-mol% BaO shows high oxide-ion conductivity of 1.1×10^{-2} mho/cm at 500°C and negligibly low electronic conductivity in air. The conductivity of this system rises abruptly at about 580°C during heating. This phenomenon is considered to be due to some configurational change of atoms in the rhombohedral phase. Perovskite-type compound $BaBiO_{3-\alpha}$ shows hole conductivity that is higher than the oxide-ion conductivity of the rhombohedral single phase. In the other range of composition, mixed phases are present, in which mixed ionic and hole conduction is observed.

High oxide-ion conduction in the rhombohedral phase is considered to be attributed to the migration of oxide ions via oxide ion vacancies as in the case of oxide-ion conduction reported previously.

References

1. E. C. SUBBARAO, P. H. SUTTER, AND J. HRIZO, *J. Amer. Ceram. Soc.* **48**, 443 (1965).
2. C. J. KEVANE, E. L. HOLVERSON, AND R. D. WATSON, *J. Appl. Phys.* **34**, 2083 (1963).

3. H. A. JOHANSEN AND J. G. GLEARY, *J. Electrochem. Soc.* **111**, 100 (1964).
4. T. H. ETSELL AND S. N. FLENGAS, *Chem. Rev.* **70**, 339 (1970).
5. T. TAKAHASHI, H. IWAHARA, AND T. ARAO, *J. Appl. Electrochem.* **5**, 187 (1975).
6. T. TAKAHASHI AND H. IWAHARA, *J. Appl. Electrochem.* **3**, 65 (1973).
7. T. TAKAHASHI, T. ESAKA, AND H. IWAHARA, *J. Appl. Electrochem.* **5**, 197 (1975).
8. T. TAKAHASHI, H. IWAHARA, AND T. NAGAI, *J. Appl. Electrochem.* **2**, 97 (1972).
9. L. G. SILLÉN, *Naturwissenschaften* **28**, 206 (1940).
10. G. GATTOW AND H. SCHRÖDER, *Z. Anorg. Allg. Chem.* **318**, 176 (1962).
11. M. G. HAPASE AND V. B. TARE, *Ind. J. Pure Appl. Phys.* **5**, 401 (1967).
12. R. S. SETHI AND H. C. GAUR, *Indian J. Chem.* **3**, 177 (1955).
13. E. M. LEVIN AND R. S. ROTH, *J. Res. Nat. Bur. Stand.* **68A**, 199 (1964).
14. T. TAKAHASHI AND H. IWAHARA, *Energy Conversion* **11**, 105 (1971).
15. H. YANAGIDA, R. J. BROOK, AND F. A. KRÖGER, *J. Electrochem. Soc.* **117**, 593 (1970).
16. H. SCHMALZRIED, *Z. Phys. Chem. N. F.* **38**, 87 (1963).
17. C. WAGNER, *Naturwissenschaften* **31**, 265 (1943).
18. L. G. SILLÉN AND B. AURIVILLIUS, *Z. Kristallogr.* **101**, 483 (1939).
19. T. NAKAMURA, S. KOSE, AND T. SATO, *J. Phys. Soc. Jap.* **31**, 1284 (1971).
20. J. TH. W. DE HAIR AND G. BLASSE, *Solid State Commun.* **12**, 727 (1973).